Journal of Zhejiang University-SCIENCE A (Applied Physics & Engineering) 2023 24(7):557-568
www.jzus.zju.edu.cn; www.springer.com/journal/11582
E-mail: jzus_a@zju.edu.cn

Research Article

https://doi.org/10.1631/jzus.A2200416

Check for updates

Numerical investigation of the effect of geosynthetic clay liner chemical incompatibility on flow and contaminant transport through a defective composite liner

Shiyuan YAO[1], Yuchao LI[1], Shan TONG[1]✉, Guannian CHEN[1,2,3], Yunmin CHEN[1]

[1]*MOE Key Laboratory of Soft Soils and Geoenvironmental Engineering, Department of Civil Engineering, Zhejiang University, Hangzhou 310058, China*
[2]*School of Civil & Environmental Engineering and Geography Science, Ningbo University, Ningbo 315211, China*
[3]*Ningbo ZCONE High-tech Co., Ltd., Ningbo 315000, China*

Abstract: A composite liner consisting of a geomembrane (GMB) and a geosynthetic clay liner (GCL) can be compromised by inorganic contaminants because of a defective GMB. When the composite liner with defective GMB is exposed to aggressive leachate conditions, the neglect of the chemical incompatibility of the GCL can potentially result in an underestimation of the leakage rate and flux through the composite liner. This paper proposed a numerical investigation on the effect of chemical incompatibility of GCL on the barrier performance of the composite liner with hole defect. Four cases with leachate solutions having varied cation valencies and ionic strengths were analyzed, in which the hydraulic conductivity of GCL was concentration-dependent. Both the effect of the chemical incompatibility of GCL and the mechanisms were analyzed. The incompatibility of GCL resulted in significant increases in leakage rate and flux through the composite liner by factors of up to 4.9 and 5.0, respectively. The incompatibility-affected area in GCL is located within 0.1 m from the center of the hole in the GMB. The coupled increase in the hydraulic conductivity of GCL and pore water concentration impacts the flux and leakage in a short period of time. With GCL chemical incompatibility considered, advection may dominate the contaminant transport through GCL.

Key words: Geosynthetic clay liner (GCL); Chemical incompatibility; Leakage; Contaminant transport; Hydraulic conductivity

1 Introduction

Liners are installed at the bottom of waste containment systems (e.g., landfills) to prevent contaminants from migrating to the surrounding environment. Composite liners, typically comprising a geomembrane (GMB) overlying a low permeability soil liner (i.e., geosynthetic clay liner (GCL) or compacted clay liner (CCL)), are commonly used in modern landfills (Rowe and Brachman, 2004; Rowe, 2012). A permeable layer or a subsoil may be constructed at the base of the composite liner, to act as an attenuation layer (AL). The most commonly used GMB in composite liners is high-density polyethylene GMB, due to its high resistance to the transport of a variety of chemicals (Thomas and Koerner, 1996). Water and contaminants can barely migrate through an intact GMB via advection, and the diffusion of inorganic contaminants through an intact GMB is negligible due to its low diffusive coefficients (i.e., approximately five orders of magnitude lower than in soils) (Rowe, 1998). However, experience has shown that defects in GMBs are almost inevitable. Rowe (2012) reported seven causes of defects in GMBs, including manufacturing and installation defects, waste placement in landfills or cleaning in leachate lagoons, and stress cracking due to the GMB aging. Thus, for a composite liner, the primary migration pathway for inorganic solutes is through defects in the GMB via advection, then through the GCL/CCL via advection and diffusion (Foose et al., 2001, 2002; Rowe, 2012).

A GCL typically comprises a thin layer of bentonite sandwiched by two layers of geotextiles with needle-punching reinforcement. The excellent containment

✉ Shan TONG, stong@zju.edu.cn
Shiyuan YAO, https://orcid.org/0000-0001-6582-0788
Shan TONG, https://orcid.org/0000-0002-6145-0721

Received Aug. 29, 2022; Revision accepted Dec. 1, 2022;
Crosschecked Mar. 31, 2023

property of GCL is attributed to the low hydraulic conductivity of the bentonite when properly hydrated. However, GCL is susceptible to chemical attack due to the incompatibility of the bentonite with aggressive leachates containing high cation valency, high ionic strength, or extreme pH. The significant increase in hydraulic conductivity of GCL (k_{GCL}) when the GCL is exposed to inorganic solutions (e.g., $k_{GCL}/k^0_{GCL}>1$, where k^0_{GCL} is the hydraulic conductivity of GCL permeated with deionized water (DIW)), has been demonstrated by extensive laboratory experiments (Petrov and Rowe, 1997; Petrov et al., 1997; Jo et al., 2001, 2004, 2005; Vasko et al., 2001; Kolstad et al., 2004; Katsumi et al., 2007). Such chemical incompatibility is one of the greatest concerns when employing GCLs in waste containment systems.

A comparison of k_{GCL} based on flexible-wall hydraulic conductivity tests with DIW and inorganic solutions with solute concentrations (c) ranging from 0.005 to 1 mol/L is shown in Fig. 1. The values of k_{GCL} vary between 9×10^{-12} and 3×10^{-11} m/s with DIW, and increase by up to 5 orders of magnitude (i.e., 5×10^{-6} m/s) with increasing solute concentrations. However, the relationship between k_{GCL} and c is nonlinear. The k_{GCL} only increases by a factor of up to 5 at dilute concentrations (i.e., $c\leqslant0.01$ mol/L), but significantly increases by 1–5 orders of magnitude at aggressive concentrations (i.e., $c>0.01$ mol/L). The k_{GCL} for the solutions with divalent cations, with most values exceeding 1×10^{-9} m/s when $c\geqslant0.025$ mol/L, generally is greater than that for the solutions with monovalent cations, with most values lower than 1×10^{-9} m/s except for NH_4Cl. The chemical compatibility can be enhanced by allowing GCLs to be hydrated with water before being exposed to chemical solutions, i.e., prehydration treatment. As shown in Fig. 1, a 1–4 orders of magnitude difference in k_{GCL} exists between prehydrated and non-prehydrated GCLs when permeated with the same solutions (Petrov and Rowe, 1997; Ruhl and Daniel, 1997; Shackelford et al., 2000; Vasko et al., 2001; Jo et al., 2004).

In previous studies the mechanism of contaminant transport in composite liners has been extensively studied by using numerical methods, and k_{GCL} is an essential parameter in the assessment of contaminant transport. Foose et al. (2002) compared the solute transport in three composite liners using a 3D numerical model, in which the values of k_{GCL} used were

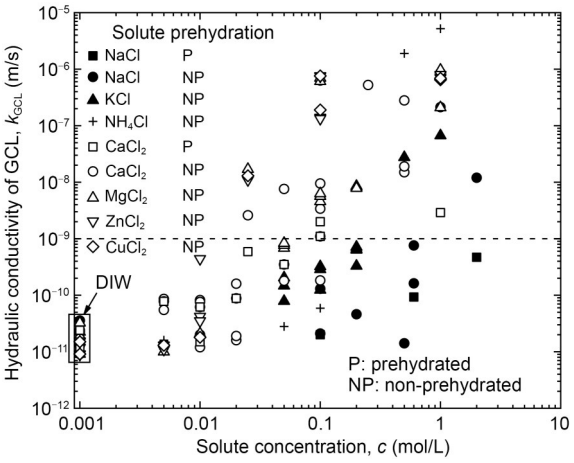

Fig. 1 Hydraulic conductivity of GCL with deionized water and inorganic solutions (Petrov and Rowe, 1997; Shackelford et al., 2000; Jo et al., 2001, 2005; Vasko et al., 2001; Lee and Shackelford, 2005; Lee et al., 2005; Katsumi et al., 2007; Setz et al., 2017; Chai and Prongmanee, 2020)

representative values for GCLs permeated with real leachate (i.e., 1×10^{-11} and 1×10^{-12} m/s). Rowe and Brachman (2004) assessed the equivalence of GCL and CCL in composite liners using a 1D model with a relatively large value of k_{GCL} of 2×10^{-10} m/s to represent the increases in k_{GCL} with leachate and suggested that the barrier systems should be designed based on a higher k_{GCL} to avoid the effect of increases in k_{GCL} when the GCL is exposed to leachate. Saidi et al. (2006) calculated the impact on flow rate and wetted area of a composite liner involving partially saturated GCL using 2D and 3D numerical models where the hydraulic conductivity of GCL was related to saturations. El-Zein et al. (2016) simulated the transport of inorganic contaminants in a triple composite liner with multiple defects using 2D numerical models, in which different values of the hydraulic conductivity of GCL were considered. Rowe and AbdelRazek (2019) analyzed the effect of hydraulic conductivity and interface transmissivity on the leakage and contaminant transport in a composite liner by using a 2D finite element model and a semi-analytical approach, in which k_{GCL} was dependent on the stress. Many of these studies considered varying k_{GCL} with different contaminant concentrations (i.e., the chemical incompatibility of GCL) in the contaminant transport modelings. However, the transient changing of k_{GCL} with increased pore concentration as contaminant migrates through the liner, and the effect of this coupled increase in both k_{GCL} and pore water concentration on the barrier performance

of composite liners has not been quantitatively investigated, as most numerical studies of contaminant transport assumed constant values of k_{GCL} in such studies.

The values of k_{GCL} adopted by Foose et al. (2002) and Rowe and Brachman (2004) were from experimental data measured by Ruhl and Daniel (1997) for GCLs permeated with a municipal solid waste (MSW) landfill leachate solution from the mid-western USA, which comprised 16 mmol/L monovalent cation (Na^+) and 9 mmol/L divalent cations (Ca^{2+} and Mg^{2+}). However, the concentrations of cations in the leachate were lower than typical values reported for MSW landfill leachates. For example, Kjeldsen et al. (2002) reported that the maximum concentrations of Na^+, Ca^{2+}, and Mg^{2+} in MSW leachates were 335, 180, and 625 mmol/L, respectively, based on the data collected from 14 MSW landfills. Higher inorganic cation concentrations also have been found for the leachates from other types of solid waste landfills, such as hazardous waste (HW) landfills and MSW ash landfills. Rowe et al. (2004) summarized the leachate characteristics of three HW landfills and six MSW ash landfills and found that the average and maximum concentrations of monovalent cations in the HW landfills were 228 and 347 mmol/L, respectively; the average concentrations of monovalent and divalent cations in MSW ash landfills were 79 and 80 mmol/L, whereas the maximum concentrations of the two types of cations were 220 and 222 mmol/L. Khodary et al. (2020) also reported a very high Na^+ concentration of 660 mmol/L in the leachate from the El-Nasreya landfill in Egypt (a hazardous waste landfill). Moreover, the use of GCL composite liners has recently extended to mining and other industrial facilities (Bouazza et al., 2014) such as solar ponds, reverse osmosis ponds, and brine ponds, in which high salt concentrations may occur. El-Sebaii et al. (2011) found that the concentration of NaCl at the bottom of a solar pond was 26%, which was roughly equivalent to 4400 mmol/L. Abdulsalam et al. (2017) reported that the Na^+ concentration in a brine pond was as high as 1000 mmol/L. Thus, the values of k_{GCL} used in most of the previous studies on contaminant transport may be relatively low and may have resulted in an underestimation of the containment properties of the GCL. In addition, it is necessary to investigate the effect of the coupled increase of k_{GCL} with c on the containment properties of long-term barriers under a high salt concentration environment.

In this paper, the effect of coupled increased k_{GCL} with c on the barrier performance of a composite liner comprising a defective GMB and a GCL is investigated with varied cation valence and ionic strength (I_0) in the permeating leachates based on a 2D numerical model. The contaminant transport process in the GCL is analyzed in terms of the changes in distributions of cation concentration, hydraulic conductivity, hydraulic head, flow rate, and total contaminant flux in GCL with time. In addition, comparisons of advective and diffusive transport of contaminants through the composite liner are also discussed.

2 Model

2.1 Geometry

A 2D axisymmetric model of a composite liner comprising a thickness-neglected GMB and a 7-mm-thick GCL, overlaying a 2-m-thick AL was established, with r representing the radial direction and z representing the vertical direction, as shown in Fig. 2. The GMB had a 5-mm-radius hole (r_h=5 mm), representing a large circular defect in the GMB (Giroud, 1997). The center of the hole was set as the origin of the coordinates, that is, r=0 m and z=0 m. The radius of the model (r_m) was set to be sufficiently wide (i.e., 6 m) to eliminate the impact of the lateral boundaries on the flow and contaminant transport simulations. The composite liner was assumed to be a saturated, homogeneous, and isotropic porous medium.

To simulate the interface leakage between the GMB and the GCL, a 0.1-mm-thin layer was added between the two layers, which was within the range of 0.02 to 0.15 mm recommended for geomembrane-soil spacing by Brown et al. (1987).

2.2 Governing equations and boundary conditions

Darcy's law and the advection-diffusion equation for porous media (Javandel et al., 1984) were used for the flow and contaminant transport simulations:

$$\nabla(k\cdot\nabla h)=0, \tag{1}$$

$$nR\frac{\partial c}{\partial t}=nD^*\cdot\nabla^2 c-\boldsymbol{u}\cdot\nabla c, \tag{2}$$

where k is the hydraulic conductivity (m/s) of the porous media; h is the total hydraulic head (m); n is the porosity; R is the retardation factor; t is the time (s);

D^* is the effective diffusion coefficient (m^2/s); $\boldsymbol{u}$ is the Darcy's velocity vector; c is the solute concentration (mol/L).

The steady-state Darcy seepage field was set as the initial flow distribution in the composite liner. The initial pore water concentration in the composite liner was assumed to be zero.

The boundary conditions of the model are shown in Fig. 2. The GMB, the axis of symmetry, and the lateral boundary were set to be no-flow boundaries for seepage and no-flux boundaries for contaminant transport. The bottom of AL was set to be a zero hydraulic head boundary for flow (corresponding to free drainage) and a zero-concentration boundary for contaminant transport (preliminary estimations had shown that the zero-concentration or zero-concentration gradient boundary of the bottom of AL had no significant impact on the result of contaminant transport in this model). The hole in the GMB was assumed to be a constant hydraulic head boundary and a constant concentration boundary. The constant hydraulic head boundary was described as follows:

$$h = h_w + H_{GCL} + H_{AL}, \tag{3}$$

where h_w is the depth of leachate (m), which was assumed to be 0.3 m in this study; H_{GCL} is the thickness of GCL (m); H_{AL} is the thickness of AL (m).

2.3 Material parameters and simulation cases

Since the leachates in HW and MSW ash and some MSW landfills contain high concentrations of inorganic cations that may induce chemical incompatibility of GCL, the source concentrations (c_0) in the modeling were selected to be 150, 300, and 600 mmol/L for NaCl and 50, 100, and 200 mmol/L for $CaCl_2$, with the same I_0 of 150, 300, and 600 mmol/L, representing low, mean, and maximum values of inorganic solute concentrations in aggressive leachates reported in the aforementioned experimental studies.

Rowe and Abdelatty (2012) reported that the effect of variations of D^* within a reasonable range on the contaminant transport through GCL was not significant. The average D^* of Na^+ and Ca^{2+} in GCL were 4.2×10^{-10} and 1.1×10^{-10} m^2/s, according to laboratory test results from Lake and Rowe (2000) and Shackelford and Lee (2003).

For the interlayer between the GMB and the GCL, the value of interface transmissivity between the GMB and GCL (θ) was assumed to be 2×10^{-11} m^2/s, in accordance with Barroso et al. (2006) and Rowe and Abdelatty (2012). Thus, the equivalent hydraulic conductivity of the GMB/GCL interface (k_{IF}) was 2×10^{-7} m/s, according to the equation proposed by Giroud and Bonaparte (1989):

$$k_{IF} = \theta / s, \tag{4}$$

where s is the thickness of interface (m).

The adsorption of Na^+ and Ca^{2+} of the clay in the composite liner was considered in this period. Hence, the retardation factors and other parameters of the materials are summarized in Table 1. The frequency of holes on the GMB was assumed to be 2.5 holes/ha, which is an appropriate value corresponding to the scenario of GMBs installed with strict construction quality assurance (Giroud and Bonaparte, 2001).

Dissolved inorganic salt is a major group of components of MSW landfill leachates, along with volatile fatty acids, heavy metals at low concentrations, and volatile organic compounds (Rowe and AbdelRazek, 2019). Since chloride was not affected by precipitation, sorption, or biodegradation (Rowe et al., 2004), NaCl and $CaCl_2$ were regarded as the representative

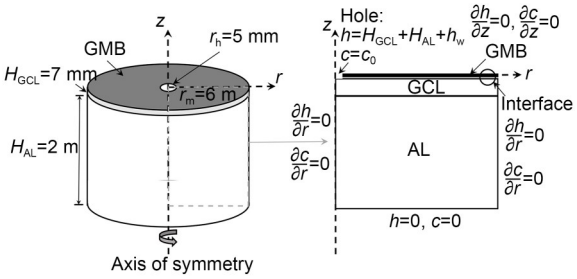

Fig. 2 Schematic of the 2D axisymmetric model of the composite liner above the AL (not in scale)

Table 1 Material parameters and transport properties of GCL and AL

Type	Porosity	Hydraulic conductivity (m/s)	Effective diffusion coefficient (m^2/s)	Retardation factor
GCL	0.7[a]	See Table 2	4.2×10^{-10} for Na^+, 1.1×10^{-10} for Ca^{2+}	9.5[b] for Na^+, 13.8[c] for Ca^{2+}
AL	0.3[a]	1.0×10^{-7}[a]	7.0×10^{-10}[a]	1

[a] Rowe and Brachman (2004); [b] Shackelford and Redmond (1995); [c] Barone et al. (1989)

inorganic contaminants with monovalent and divalent cations in this paper. Two sets of k_{GCL}-c data from experimental studies in the literature were selected for the simulations (Fig. 3). All the k_{GCL} values used in this paper were measured after chemical equilibrium in the corresponding hydraulic conductivity tests had been achieved, and thus can be adopted as the long-term k_{GCL} with salt solutions (Jo et al., 2005). As shown in Fig. 3, a logistic function was adopted to describe the relationship between the measured k_{GCL} and c:

$$k_{GCL}=k_{GCL}^{\infty}+\frac{k_{GCL}^{0}-k_{GCL}^{\infty}}{1+(c/m)^{a}}, \tag{5}$$

where k_{GCL}^{∞} is the maximum value of k_{GCL} corresponding to the highest permeant concentration, k_{GCL}^{0} is the initial k_{GCL} in all cases (i.e., hydraulic conductivity of GCL permeated with DIW), m is the value of c corresponding to $k_{GCL}=(k_{GCL}^{0}+k_{GCL}^{\infty})/2$, and a is a parameter related to the range of c in which the k_{GCL} varies dramatically. Values of k_{GCL}^{0}, k_{GCL}^{∞}, m, and a in the incompatible cases are summarized in Table 2. For all cases, k_{GCL}^{0} was assumed to be 1×10^{-11} m/s, which represented the value for DIW reported in (Ruhl and Daniel, 1997; Foose et al., 2001). In the two cases considering chemical incompatibility, as k_{GCL} was assumed related to the porewater concentration in GCL based on Eq. (5), k_{GCL} increased over time as the porewater concentration in GCL increased over time. As

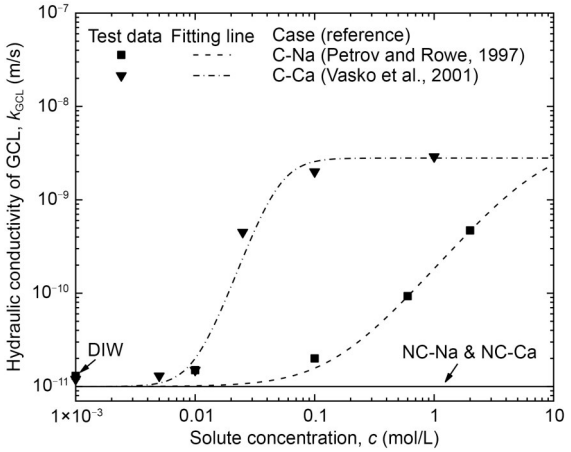

Fig. 3 Hydraulic conductivity of prehydrated GCLs with NaCl or $CaCl_2$ solution. C-Na represents the cases of prehydrated GCL permeated with NaCl; C-Ca represents the cases of prehydrated GCL permeated with $CaCl_2$; NC-Na and NC-Ca represent two cases without consideration of incompatibility. dots: experimentally measured data from the literature; lines: fitting curves of each set of data based on Eq. (5)

Table 2 Simulation cases and values for parameters

Case	Migrating solute	Parameter			
		k_{GCL}^{0} (m/s)	k_{GCL}^{∞} (m/s)	m	a
NC-Na	NaCl	1.0×10^{-11}	1.0×10^{-11}	–	–
C-Na	NaCl	1.0×10^{-11}	4.1×10^{-9}	8.0	1.5
NC-Ca	$CaCl_2$	1.0×10^{-11}	1.0×10^{-11}	–	–
C-Ca	$CaCl_2$	1.0×10^{-11}	2.8×10^{-9}	0.05	3.5

the concentration in GCL increases over time in the simulation process, in the cases of NC-Na and NC-Ca, k_{GCL} was assumed to be constant (i.e., $k_{GCL}=k_{GCL}^{0}=1\times10^{-11}$ m/s) throughout the modeling.

2.4 Numerical method

A commercial finite element software, COMSOL Multiphysics, was used to establish the 2D axisymmetric model to simulate the coupled transient flow and contaminant transport in the composite liner. The numerical method used in this study for the coupled advection-diffusion transport process was validated by simulating the long-term effluent concentration curves of the chemical transport column tests, which had been performed by the authors (Chen et al., 2020, 2022). The numerical method used in this study was also verified by comparison with the numerical results obtained by Foose et al. (2002) and Rowe and Abdelatty (2012) for leakage and long-term solute transport through composite liners with a constant hydraulic conductivity for GCL. A steady-state flow field simulation was conducted first with the initial value of k_{GCL}, then the result of steady-state flow velocity was used as the initial value in the next transient simulation of both flow and contaminant transport fields, in which the non-linear k_{GCL}-c relationship from the unit tests of GCL chemical compatibility was incorporated based on Eq. (5). The configuration of triangular finite element grids applied to the model is shown in Fig. 4. The grids near the hole and in thin layers (i.e., the GCL and the GMB/GCL interface) were refined to improve accuracy. The grid sizes in the interface layer near the hole were no larger than 0.05 mm, whereas those in the rest of the interface layer were gradually getting coarser but no larger than 0.1 mm. The grid sizes in the GCL layer were refined to be no larger than 1 mm since the thickness of GCL is relatively thin compared to that of the AL. Overall, the configuration of grids contained 761 653 elements and 402 335 nodes. Two dependent variables, i.e., pore water pressure and solute concentration, were defined for each

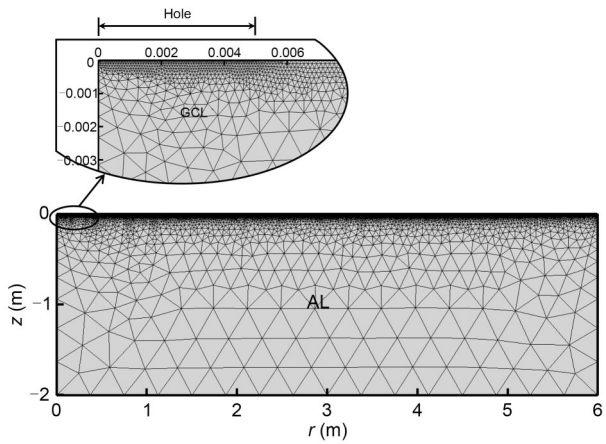

Fig. 4 Configuration of the finite element grids applied to the model

node. A time-dependent solver was applied with a backward differential equation for time stepping.

3 Results and discussion

3.1 Impact of chemical incompatibility on the leakage rate and contaminant flux

Typically, the average service life expectancy of a landfill will not exceed 50 years. Thus, the steady-state value of leakage rate (Q) and total flux (J_t) of Na^+ or Ca^{2+} through the GCL at t=50 a for all four cases were calculated to analyze the impact of the chemical incompatibility on the barrier performance of the composite liner, as shown in Figs. 5a and 5b.

In the two cases with incompatibility considered, the values of Q ranged between 0.021 and 0.094 lphd (liters per hectare per day, 1 lphd=1.16×10^{-8} $m^3/(ha\cdot s)$), which are 1.1 to 4.9 times higher than those for the four cases with incompatibility neglected (i.e., 0.019 lphd for NC-Na and NC-Ca). In the cases with NaCl solutions, compared to the NC-Na and NC-Ca cases, Q for the C-Na and C-Ca cases increased by a factor of 1.1 to 1.5, and 3.5 to 4.9, respectively, as I_0 increased from 150 to 600 mmol/L. Thus, the neglect of GCL incompatibility will probably result in a considerable underestimation of Q.

When incompatibility is considered, the increased values of Q with increasing I_0 for the Ca^{2+} cases are higher than those for the Na^+ cases, which can be attributed to the higher k_{GCL} with $CaCl_2$ solutions relative to that with NaCl solutions at the same I_0. For example,

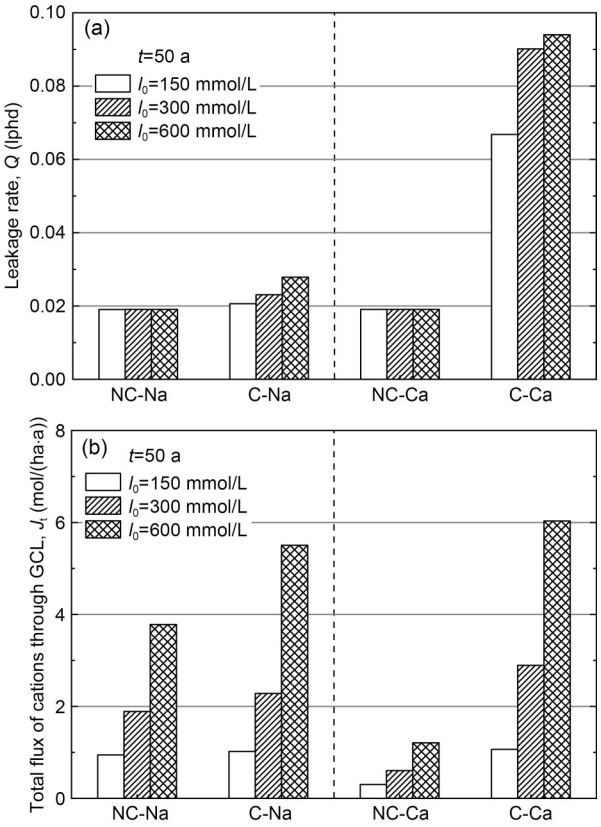

Fig. 5 Leakage rate Q (a) and total flux of cations through the GCL (J_t) (b) at t=50 a for all four cases

when I_0=300 mmol/L, Q for C-Ca was 3.9 times higher than that for C-Na since the value of k_{GCL} of the former was 65 times higher than that of the latter.

For the GCL, the J_t is a function of both k_{GCL} and I_0. For NC-Na and NC-Ca cases, J_t increased from 0.95 to 3.78 mol/(ha·a) and from 0.30 to 1.21 mol/(ha·a), respectively, as I_0 increased from 150 to 600 mmol/L. When incompatibility was considered, J_t for most cases significantly increased. As I_0 increased from 150 to 600 mmol/L, the values of J_t for C-Na cases increased by a factor of 1.1 to 1.5 relative to that for NC-Na cases, whereas those for C-Ca cases were 3.5 to 5.0 times higher than that for the NC-Ca case. For every case, the increases in J_t were almost identical to Q.

In general, values of J_t for Ca^{2+} cases were higher than those for Na^+ cases at the same I_0. For example, when I_0=300 mmol/L, J_t for C-Ca was 2.9 mol/(ha·a), whereas that for C-Na was 2.3 mol/(ha·a), smaller than the former, although the concentration of Na^+ was three times higher than that of Ca^{2+}. The impact of cation valence on chemical incompatibility is more significant than that of cation concentration.

In summary, for composite liners, the chemical incompatibility of GCL may induce considerable increases of Q and J_t when the GCL is exposed to aggressive leachates from MSW landfills with high concentration levels, as well as HW and MSW ash landfills. It is necessary to consider the incompatibility of GCL when evaluating the barrier performance of composite liners.

3.2 Mechanisms of flow and contaminant transport affected by chemical incompatibility

In this section, the contribution of GCL incompatibility in the mechanism of flow and contaminant transport through the composite liner is investigated mainly by comparing the cases of C-Ca and NC-Ca at c_0=100 mmol/L, which represents the mean value of divalent cation concentration for typical aggressive leachates in MSW ash landfills.

In the simulation, the concentration of Ca^{2+} in the GCL was nearly identical along the vertical direction after 0.1 a since the GCL was very thin compared to the AL. Thus, the concentration profiles at the mid-depth of GCL were used to represent the concentration distribution in the whole GCL at varying service durations (0.01 to 50 a), for C-Ca with c_0=100 mmol/L. As shown in Fig. 6, the concentration beneath the hole rapidly increased to c_0 within 0.1 a, more accurately, on the fifth day, as shown by the difference between the line of t=0.01 a and t=0.1 a.

In the radial direction, the Ca^{2+} concentration gradually decreased as r increased, and varied significantly with time. The r corresponding to c=0.95c_0 (that is, c=95 mmol/L in this case) increased from 0.02 (four times of r_h) to 0.06 m (12 times of r_h), and the r corresponding to c=0.01c_0 (that is, c=1 mmol/L in this case) increased from 0.03 to 2.4 m when t increased from 0.1 to 50 a. It can be inferred that in the zone where c decreased rapidly, the radial concentration gradient decreased with time as the contaminant continuously migrated along the radial direction.

The varying radial profile of k_{GCL} with time at the mid-depth of GCL for C-Ca with c_0=100 mmol/L is shown in Fig. 7. When chemical incompatibility was considered, k_{GCL} was assumed to be dependent on c (data of C-Ca case in Fig. 3). Moreover, k_{GCL} increases nonlinearly with c as the increase reduces at higher c. Thus, the portion of GCL where c was close to c_0 (dozens of r_h in the radial direction) had a k_{GCL} almost identical to $k_{GCL}^{c_0}$ (value of k_{GCL} corresponding to c_0) and probably would have poor barrier performance. A deterioration zone (D Zone) can be defined to represent the portion where $k_{GCL}/k_{GCL}^{c_0}$>0.9 at t=0.1 a. For the portion far away from the hole, c remained low and k_{GCL} was close to k_{GCL}^0 (i.e., 1×10^{-11} m/s) at t⩽50 a. A non-impact zone (NI Zone) was defined to represent the portion where k_{GCL}/k_{GCL}^0<1.1 at t=50 a. The portion between the D Zone and the NI Zone was defined as a sub-deterioration zone (SD Zone), in which the k_{GCL} considerably increased during t=0.1–50 a. For C-Ca, the radial lengths of D Zone, SD Zone, and NI Zone were 0.03, 1.47, and 4.50 m, respectively (Fig. 7). In this study, the radii of D Zone and SD Zone in all the cases were smaller than 0.05 and 3 m, respectively. Thus, when chemical incompatibility is considered,

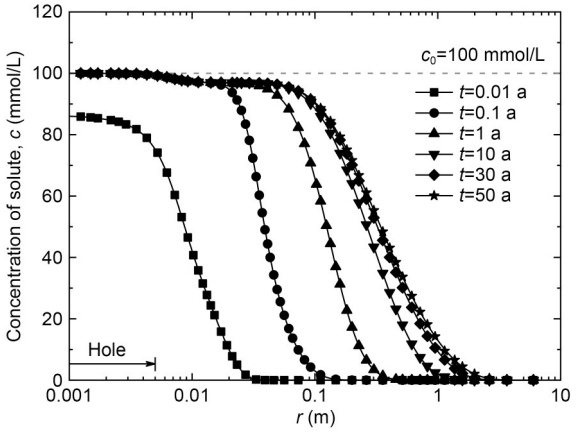

Fig. 6 Ca^{2+} concentration profiles at the mid-depth of GCL for C-Ca with c_0=100 mmol/L

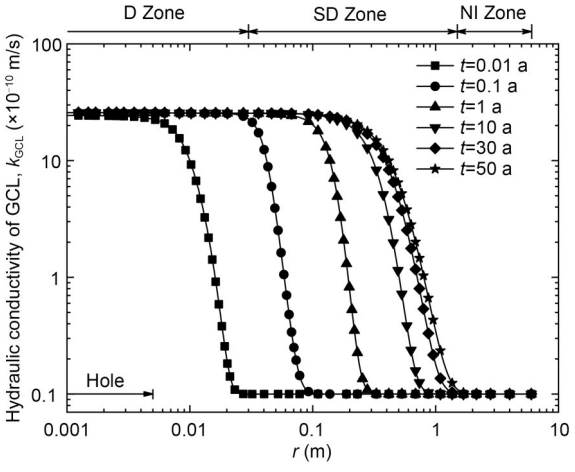

Fig. 7 k_{GCL} profiles at the mid-depth of GCL for C-Ca with c_0=100 mmol/L

the affected region of hydraulic conductivity in GCL is very small for a hole frequency in GMB of 2.5 hole/ha.

The distribution profiles of the hydraulic head in the D Zone (r⩽0.03 m) of the GCL for the cases of NC-Ca and C-Ca at c_0=100 mmol/L are shown in Fig. 8. For the NC-Ca case, the head distribution within the GCL remained constant over time, as shown in Fig. 8a. For the C-Ca case, the head distribution changed rapidly in the first 0.1 years, resulting in an increased radial hydraulic gradient in the D Zone, and then remained nearly unchanged with time, as shown in Figs. 8b–8d. The denser contour lines of the C-Ca case indicated that the hydraulic gradient near the hole was higher than in the NC-Ca case. The radial drop of the head occurred mainly within the D Zone for both cases, but was more significant for the C-Ca case. Beyond the D zone (r⩾0.03 m), the head for the NC-Ca case was lower than 1.073 m whereas that for the C-Ca case was lower than 0.075 m, corresponding to 47% and 3% of the initial head (i.e., 2.307 m), respectively.

The incompatibility of GCL can induce a narrower wetted area, where GMB-GCL interface flow occurs (Giroud and Bonaparte, 1989; Rowe 1998). In this model, the wetted area was defined as the area where the hydraulic head at steady-state was no less than 10% of the original value. For the NC-Ca and C-Ca cases, the radii of the wetted area (R_w) were 0.14 m and 0.02 m, respectively. The effect of GCL incompatibility on R_w can be explained by the analytical solution proposed by Giroud and Bonaparte (1989):

$$k_s = \frac{4\theta h_w}{R_w^2[\,2\ln(R_w/r_h)-1\,]+r_h^2}, \tag{6}$$

where k_s is the equivalent hydraulic conductivity of the underlying soil. R_w is inversely related to k_s which is also related to k_{GCL}. Thus, higher k_{GCL} would result in smaller R_w.

For the NC-Ca case, since k_{GCL} (i.e., 1×10^{-11} m/s) was much lower than the hydraulic conductivity of AL (i.e., 1×10^{-7} m/s), the reduction of the hydraulic head in the vertical direction mainly occurred in the GCL (approximately reduced by 99.1%) and resulted in a value of 0.002 m at the base of GCL beneath the hole. For the C-Ca case, the maximum hydraulic head at the base of GCL was 0.079 m, a little higher than NC-Ca because of higher k_{GCL}.

Following the analyses of k_{GCL} and the hydraulic head, the profile of flow rate per unit area (q) at the mid-depth of GCL is shown in Fig. 9. Compared with the NC-Ca case, the increased k_{GCL} for the C-Ca case resulted in significantly higher q in the D Zone and a more rapid radial decrease along the radial distance. The maximum value of q for the C-Ca case (8.1×10^{-7} m/s) was nearly 2.5 orders of magnitude greater than that for the NC-Ca case (3.3×10^{-9} m/s). The estimated radial cumulative flow rate indicated that 88% of the leakage occurred within the D Zone (r⩽0.03 m) for the C-Ca case, whereas the range of the same proportion of leakage rate for the NC-Ca case was 0.36 m, more than 10 times larger than the former. Thus, the incompatibility of GCL induces a higher amount of flow beneath the hole.

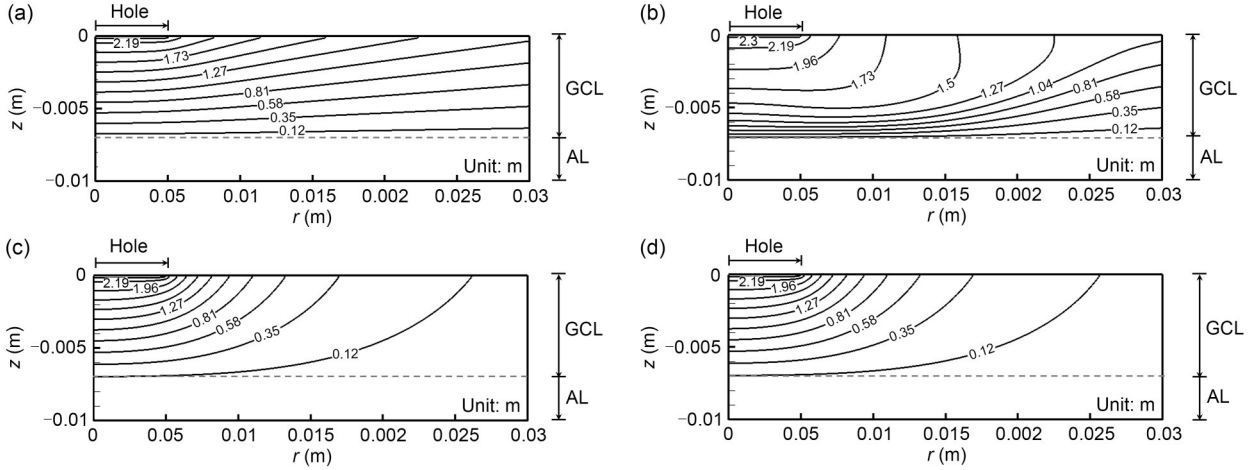

Fig. 8 Contours of hydraulic head in the GCL for NC-Ca and C-Ca with c_0=100 mmol/L: (a) NC-Ca; (b) C-Ca, t=0.01 a; (c) C-Ca, t=0.1 a; (d) C-Ca, t=50 a

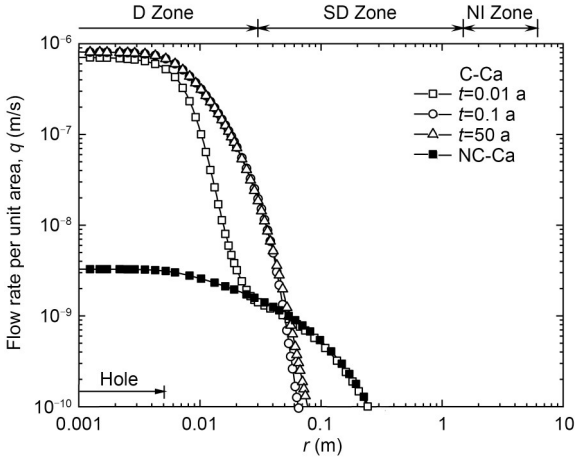

Fig. 9 Profiles of flow rate at the mid-depth of GCL for NC-Ca and C-Ca with c_0=100 mmol/L

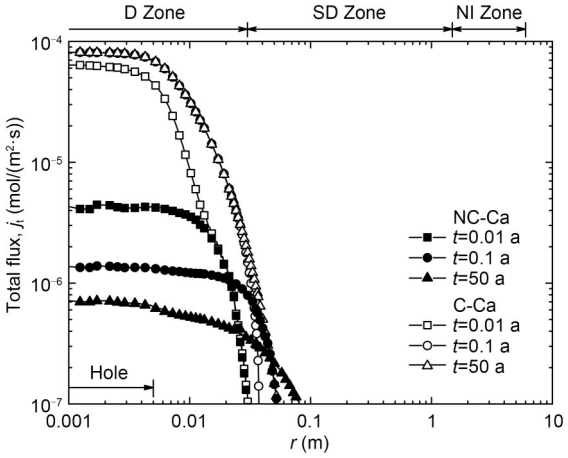

Fig. 10 Total flux profiles of Ca^{2+} through the unit area of mid-depth of GCL for NC-Ca and C-Ca with c_0=100 mmol/L

For the C-Ca case, the distribution of q maintained constant after 0.1 a due to the rapid increase of k_{GCL}, so that q reached a steady state. In this case, the effect of the coupled increase in k_{GCL} and c occurred rapidly (less than 0.1 a). Similar results have also been found for the C-Na cases. However, the flow rate distribution for C-Na cases (which is not show in Fig. 9) showed that q kept gradually increasing for 10 years for C-Na cases even though it exceeded 98% of the steady-state value after 1 a.

For all cases with incompatibility of GCL considered, the high values of q (>10% of the maximum value) that occurred within the area of r<0.1 m were larger than in the D Zone but smaller than in the combined area of D Zone and SD Zone. Thus, according to the seepage, the actual incompatibility-affected area in the GCL was located within 0.1 m from the center of the hole in the GCL.

The distributions of the total flux of Ca^{2+} through the unit area of mid-depth of GCL (j_t) with time are shown in Fig. 10. The trend of decreasing j_t with increasing r was similar to that of q with r. The maximum j_t for the C-Ca case (8.1×10^{-5} mol/(m^2·s)) was approximately two orders of magnitude greater than that for the NC-Ca case (7.1×10^{-7} mol/(m^2·s)) at t=50 a, and j_t for the C-Ca case decreased more than three orders of magnitude with r=0.1 m. For all the cases where the incompatibility of GCL was considered, the high values of j_t (>10% of the maximum value) also occurred within the area of r<0.1 m, indicating that the radius of the actual incompatibility-affected area in the GCL was smaller than 0.1 m according to contaminant transport, which was the same as q.

For the C-Ca case, j_t increased over time in all zones because of the increased k_{GCL}. The change in the distribution of j_t was minimal after 0.1 a, indicating that the flux through GCL reached a steady-state within a very short time, the same as the change in q. For all the other three cases, the change in the distribution of j_t was very small after one year. Therefore, both the analyses for the change of q and j_t over time indicated that consideration of the coupled increase in k_{GCL} and c had a limited impact on leakage rate and contaminant flux, so it can be ignored for a rapid evaluation of barrier performance of composite liners.

Based on the analyses of q and j_t, neglect of the incompatibility of GCL will cause significant underestimation of the wetted area and of the leakage and flux occurring beneath the hole, leading to a considerably unconservative prediction of both the flow and the contaminant barrier performances of the composite liner.

The total flux is the combination of advective and diffusive fluxes when the impact of dispersion is ignored. The integrals of advective flux and diffusive flux through the composite liner (J_a and J_d) are defined as

$$\begin{cases} J_a = \int_0^{r_m} qc \times 2\pi r \mathrm{d}r, \\ J_d = \int_0^{r_m} -nD^* \dfrac{\partial c}{\partial z} \times 2\pi r \mathrm{d}r. \end{cases} \tag{7}$$

The fluxes of all cases reached a steady-state (>95% of the maximum values) within 20 years. The steady-state values of J_a and J_d for all four cases with I_0 ranging from 150 to 600 mmol/L are summarized

in Table 3. The downward direction was regarded as positive for fluxes. For cases with incompatibility neglected, the values of J_a were slightly smaller than that of J_d with the difference remaining less than 20%, indicating that diffusion was comparable to advection in the contaminant transport. Moreover, the ratio of J_a and J_d ($|J_a/J_d|$) was not affected by c_0 if the incompatibility of GCL was neglected.

Table 3 Steady-state values of advective and diffusive fluxes through the composite liner

Case	I_0 (mmol/L)	$k_{GCL}^{c_0}$ ($\times10^{-11}$ m/s)	J (mol/(ha·a))		$\lvert J_a/J_d\rvert$
			J_a	J_d	
NC-Na	150	1.0	0.41	0.54	0.8
	300	1.0	0.82	1.07	0.8
	600	1.0	1.64	2.14	0.8
C-Na	150	2.0	0.54	0.48	1.1
	300	4.0	1.48	0.80	1.8
	600	9.2	4.55	0.96	4.7
NC-Ca	150	1.0	0.14	0.16	0.8
	300	1.0	0.28	0.33	0.8
	600	1.0	0.55	0.65	0.8
C-Ca	150	140	1.18	−0.12[a]	10.1
	300	260	3.20	−0.31	10.3
	600	280	6.69	−0.66	10.1

[a] The negative sign represents the transport in an upward direction (from the GCL/AL interface back into the GCL)

Higher $k_{GCL}^{c_0}$ resulted in higher J_a and J_d, as expected. With incompatibility considered, the values of J_a significantly increased from 1.3 to 12.2 times. For case C-Na with the least affected $k_{GCL}^{c_0}$ (as low as 2×10^{-11} m/s), J_a was 1.1 times higher than J_d. Therefore, when $k_{GCL}^{c_0}$ is higher than 2×10^{-11} m/s, J_a will exceed J_d, and the value of $|J_a/J_d|$ increases with the increasing $k_{GCL}^{c_0}$. For C-Na cases, the values of $|J_a/J_d|$ ranged from 1.1 to 4.7; advection had a greater impact than diffusion and the share of advection increased as I_0 increased. For C-Ca cases, the values of $|J_a/J_d|$ ranged from 10.1 to 10.3, indicating that the contaminant transport in GCL was dominated by advection in Ca^{2+} cases.

For cases with high $k_{GCL}^{c_0}$ (i.e., C-Ca cases), the direction of J_d was opposite to J_a. In those cases, a small wetted area resulted in a small region with very high c beneath the hole in AL, and the contaminant transport along the radial direction was faster in AL than that in GCL due to the higher hydraulic conductivity of the AL. Thus, in a region near the hole, c in AL was higher than in GCL along the vertical direction, and a negative concentration gradient occurred across the boundary between GCL and AL. However, J_a in those cases was more than one order of magnitude higher than J_d, and thus the contaminant transport was dominated by advection.

Note that the presence of AL beneath the GCL composite liner could significantly reduce the contaminant flux, especially the advective flux because the large thickness of the AL could significantly reduce the concentration of contaminant in the region beneath the hole. For all cases, total fluxes of Ca^{2+} or Na^{+} through the mid-depth of AL decreased by 43% to 46% compared to those through the liner, respectively, with advective fluxes decreasing by more than 95%.

4 Conclusions

The effect of chemical incompatibility of GCL on the barrier performance of defective composite liners was investigated numerically via a comparison of four cases. The mechanism of the effect was analyzed in terms of the distributions of contaminant concentration, hydraulic conductivity, hydraulic head, flow rate, and contaminant flux. The following conclusions were drawn based on the analyses and comparisons.

It is necessary to consider the chemical incompatibility of GCL when evaluating barrier performance of composite liners with defective GMB, especially for a landfill with leachates containing high concentrations of inorganic cations. In this study, as the ionic strength of inorganic solutions increased from 150 to 600 mmol/L, the leakage rate and the total flux through the composite liner increased by a factor of 1.1 to 1.5 for C-Na cases, and 3.5 to 4.9 for C-Ca cases within the average duration of life expectancy of a landfill (t=50 a). The increase of k_{GCL} due to chemical incompatibility results in a much higher flow rate and flux in the GCL portion directly beneath the hole, and it also results in a smaller radius of the wetted area. Compared to the NC-Ca cases, the C-Ca cases have much more leakage within the D Zone. For all the cases considering the incompatibility, the radii of the incompatibility-affected area in GCL were less than 0.1 m. The increasing process of k_{GCL} occurs in a short period of time (less than 1 a for the cases in this study) if the chemical incompatibility of GCL is considered. The chemical incompatibility of GCL significantly increases the

ratio of advective flux to diffusive flux through the defective composite liner.

This paper focused on the effect of the GCL chemical incompatibility on the barrier performance of composite liners. The effects of other parameters, such as the size of the hole, the interface transmissivity, and the AL thickness, were not considered here but can be evaluated in the future based on this paper. The numerical method in this paper can be used in the future to design and simulate in-site tests of contaminant transport through defective composite liners.

Acknowledgments

This work is supported by the National Key Research and Development Program of China (Nos. 2018YFC1802304 and 2019YFC1806002) and the National Natural Science Foundation of China (Nos. 42077241 and 51988101).

Author contributions

Shiyuan YAO and Yuchao LI designed the research. Shiyuan YAO and Guannian CHEN processed the corresponding data. Shiyuan YAO and Shan TONG wrote the first draft of the manuscript. Yuchao LI and Yunmin CHEN helped to organize the manuscript. Shan TONG revised and edited the final version.

Conflict of interest

Shiyuan YAO, Yuchao LI, Shan TONG, Guannian CHEN, and Yunmin CHEN declare that they have no conflict of interest.

References

Abdulsalam A, Idris A, Mohamed TA, et al., 2017. An integrated technique using solar and evaporation ponds for effective brine disposal management. *International Journal of Sustainable Energy*, 36(9):914-925. https://doi.org/10.1080/14786451.2015.1135923

Barone FS, Yanful EK, Quigley RM, et al., 1989. Effect of multiple contaminant migration on diffusion and adsorption of some domestic waste contaminants in a natural clayey soil. *Canadian Geotechnical Journal*, 26(2):189-198. https://doi.org/10.1139/t89-028

Barroso M, Touze-Foltz N, von Maubeuge K, et al., 2006. Laboratory investigation of flow rate through composite liners consisting of a geomembrane, a GCL and a soil liner. *Geotextiles and Geomembranes*, 24(3):139-155. https://doi.org/10.1016/j.geotexmem.2006.01.003

Bouazza A, Singh RM, Rowe RK, et al., 2014. Heat and moisture migration in a geomembrane–GCL composite liner subjected to high temperatures and low vertical stresses. *Geotextiles and Geomembranes*, 42(5):555-563. https://doi.org/10.1016/j.geotexmem.2014.08.002

Brown KW, Thomas JC, Lytton RL, et al., 1987. Quantification of Leak Rates Through Holes in Landfill Liners. EPA/600/S2-87/062, U.S. Environmental Protection Agency, Hazardous Waste Engineering Research Laboratory, Cincinnati, USA.

Chai JC, Prongmanee N, 2020. Barrier properties of a geosynthetic clay liner using polymerized sodium bentonite. *Geotextiles and Geomembranes*, 48(3):392-399. https://doi.org/10.1016/j.geotexmem.2019.12.010

Chen GN, Li YC, Zuo XR, et al., 2020. Comparison of adsorption behaviors of kaolin from column and batch tests: concept of dual porosity. *Journal of Environmental Engineering*, 146(9):04020102. https://doi.org/10.1061/(ASCE)EE.1943-7870.0001792

Chen GN, Yao SY, Wang Y, et al., 2022. Measurement of contaminant adsorption on soils using cycling modified column tests. *Chemosphere*, 294:133822. https://doi.org/10.1016/j.chemosphere.2022.133822

El-Sebaii AA, Ramadan MRI, Aboul-Enein S, et al., 2011. History of the solar ponds: a review study. *Renewable and Sustainable Energy Reviews*, 15(6):3319-3325. https://doi.org/10.1016/j.rser.2011.04.008

El-Zein A, McCarroll I, Masoudian MS, 2016. Inorganic transport through composite geosynthetics and compacted clay liners under geomembranes with multiple defects. *Australian Geomechanics Journal*, 51(1):23-39.

Foose GJ, Benson CH, Edil TB, 2001. Analytical equations for predicting concentration and mass flux from composite liners. *Geosynthetics International*, 8(6):551-575. https://doi.org/10.1680/gein.8.0206

Foose GJ, Benson CH, Edil TB, 2002. Comparison of solute transport in three composite liners. *Journal of Geotechnical and Geoenvironmental Engineering*, 128(5):391-403. https://doi.org/10.1061/(asce)1090-0241(2002)128:5(391)

Giroud JP, 1997. Equations for calculating the rate of liquid migration through composite liners due to geomembrane defects. *Geosynthetics International*, 4(3-4):335-348. https://doi.org/10.1680/gein.4.0097

Giroud JP, Bonaparte R, 1989. Leakage through liners constructed with geomembranes—part II. Composite liners. *Geotextiles and Geomembranes*, 8(2):71-111. https://doi.org/10.1016/0266-1144(89)90022-8

Giroud JP, Bonaparte R, 2001. Geosynthetics in liquid-containing structures. *In*: Rowe RK (Ed.), Geotechnical and Geoenvironmental Engineering Handbook. Springer, Boston, USA, p.789-824. https://doi.org/10.1007/978-1-4615-1729-0_26

Javandel I, Doughty C, Tsang CF, 1984. Groundwater Transport: Handbook of Mathematical Models. American Geophysical Union, Washington, USA, p.228. https://doi.org/10.1029/wm010

Jo HY, Katsumi T, Benson CH, et al., 2001. Hydraulic conductivity and swelling of nonprehydrated GCLs permeated with single-species salt solutions. *Journal of Geotechnical and Geoenvironmental Engineering*, 127(7):557-567. https://doi.org/10.1061/(asce)1090-0241(2001)127:7(557)

Jo HY, Benson CH, Edil TB, 2004. Hydraulic conductivity and cation exchange in non-prehydrated and prehydrated bentonite permeated with weak inorganic salt solutions. *Clays and Clay Minerals*, 52(6):661-679. https://doi.org/10.1346/ccmn.2004.0520601

Jo HY, Benson CH, Shackelford CD, et al., 2005. Long-term hydraulic conductivity of a geosynthetic clay liner permeated with inorganic salt solutions. *Journal of Geotechnical and Geoenvironmental Engineering*, 131(4):405-417. https://doi.org/10.1061/(asce)1090-0241(2005)131:4(405)

Katsumi T, Ishimori H, Ogawa A, et al., 2007. Hydraulic conductivity of nonprehydrated geosynthetic clay liners permeated with inorganic solutions and waste leachates. *Soils and Foundations*, 47(1):79-96. https://doi.org/10.3208/sandf.47.79

Khodary SM, Elwakil AZ, Fujii M, et al., 2020. Effect of hazardous industrial solid waste landfill leachate on the geotechnical properties of clay. *Arabian Journal of Geosciences*, 13(15):706. https://doi.org/10.1007/s12517-020-05699-8

Kjeldsen P, Barlaz MA, Rooker AP, et al., 2002. Present and long-term composition of MSW landfill leachate: a review. *Critical Reviews in Environmental Science and Technology*, 32(4):297-336. https://doi.org/10.1080/10643380290813462

Kolstad DC, Benson CH, Edil TB, 2004. Hydraulic conductivity and swell of nonprehydrated geosynthetic clay liners permeated with multispecies inorganic solutions. *Journal of Geotechnical and Geoenvironmental Engineering*, 130(12):1236-1249. https://doi.org/10.1061/(asce)1090-0241(2004)130:12(1236)

Lake CB, Rowe RK, 2000. Diffusion of sodium and chloride through geosynthetic clay liners. *Geotextiles and Geomembranes*, 18(2-4):103-131. https://doi.org/10.1016/s0266-1144(99)00023-0

Lee JM, Shackelford CD, 2005. Impact of bentonite quality on hydraulic conductivity of geosynthetic clay liners. *Journal of Geotechnical and Geoenvironmental Engineering*, 131(1):64-77. https://doi.org/10.1061/(asce)1090-0241(2005)131:1(64)

Lee JM, Shackelford CD, Benson CH, et al., 2005. Correlating index properties and hydraulic conductivity of geosynthetic clay liners. *Journal of Geotechnical and Geoenvironmental Engineering*, 131(11):1319-1329. https://doi.org/10.1061/(asce)1090-0241(2005)131:11(1319)

Petrov RJ, Rowe RK, 1997. Geosynthetic clay liner (GCL)-chemical compatibility by hydraulic conductivity testing and factors impacting its performance. *Canadian Geotechnical Journal*, 34(6):863-885. https://doi.org/10.1139/t97-055

Petrov RJ, Rowe RK, Quigley RM, 1997. Selected factors influencing GCL hydraulic conductivity. *Journal of Geotechnical and Geoenvironmental Engineering*, 123(8):683-695. https://doi.org/10.1061/(asce)1090-0241(1997)123:8(683)

Rowe RK, 1998. Geosynthetics and the minimization of contaminant migration through barrier systems beneath solid waste. Proceedings of the 6th International Conference on Geosynthetics, p.27-103.

Rowe RK, 2012. Short- and long-term leakage through composite liners. The 7th Arthur Casagrande Lecture. *Canadian Geotechnical Journal*, 49(2):141-169. https://doi.org/10.1139/t11-092

Rowe RK, Brachman RWI, 2004. Assessment of equivalence of composite liners. *Geosynthetics International*, 11(4):273-286. https://doi.org/10.1680/gein.2004.11.4.273

Rowe RK, Abdelatty K, 2012. Modeling contaminant transport through composite liner with a hole in the geomembrane. *Canadian Geotechnical Journal*, 49(7):773-781. https://doi.org/10.1139/t2012-038

Rowe RK, AbdelRazek AY, 2019. Effect of interface transmissivity and hydraulic conductivity on contaminant migration through composite liners with wrinkles or failed seams. *Canadian Geotechnical Journal*, 56(11):1650-1667. https://doi.org/10.1139/cgj-2018-0660

Rowe RK, Quigley RM, Brachman RWI, et al., 2004. Barrier Systems for Waste Disposal Facilities, Edition. CRC Press, London, UK, p.45-99. https://doi.org/10.1680/gein.2004.11.4.273

Ruhl JL, Daniel DE, 1997. Geosynthetic clay liners permeated with chemical solutions and leachates. *Journal of Geotechnical and Geoenvironmental Engineering*, 123(4):369-381. https://doi.org/10.1061/(asce)1090-0241(1997)123:4(369)

Saidi F, Touze-Foltz N, Goblet P, 2006. 2D and 3D numerical modelling of flow through composite liners involving partially saturated GCLs. *Geosynthetics International*, 13(6):265-276. https://doi.org/10.1680/gein.2006.13.6.265

Setz MC, Tian K, Benson CH, et al., 2017. Effect of ammonium on the hydraulic conductivity of geosynthetic clay liners. *Geotextiles and Geomembranes*, 45(6):665-673. https://doi.org/10.1016/j.geotexmem.2017.08.008

Shackelford CD, Redmond PL, 1995. Solute breakthrough curves for processed kaolin at low flow rates. *Journal of Geotechnical and Geoenvironmental Engineering*, 121(1):17-32. https://doi.org/10.1061/(asce)0733-9410(1995)121:1(17)

Shackelford CD, Lee JM, 2003. The destructive role of diffusion on clay membrane behavior. *Clays and Clay Minerals*, 51(2):186-196. https://doi.org/10.1346/ccmn.2003.0510209

Shackelford CD, Benson CH, Katsumi T, et al., 2000. Evaluating the hydraulic conductivity of GCLs permeated with non-standard liquids. *Geotextiles and Geomembranes*, 18(2-4):133-161. https://doi.org/10.1016/s0266-1144(99)00024-2

Thomas RW, Koerner RM, 1996. Advances in HDPE barrier walls. *Geotextiles and Geomembranes*, 14(7-8):393-408. https://doi.org/10.1016/0266-1144(96)00024-6

Vasko SM, Jo HY, Benson CH, et al., 2001. Hydraulic conductivity of partially prehydrated geosynthetic clay liners permeated with aqueous calcium chloride solutions. Proceedings of the Geosynthetics Conference 2001, p.685-699.